



Research Article




Metal-chelated biomaterial from collagen extracted from pleco skin (*Pterygoplichthys pardalis*)

Amet Ovando-Roblero¹  · Rocío Meza-Gordillo¹  · Daniel Castañeda-Valbuena¹  · José Humberto Castañón-González¹  · Víctor Manuel Ruiz-Valdiviezo¹  · Rodrigo Gutiérrez-Santiago¹  · Alicia Grajales-Lagunes² 

Received: 9 November 2022 / Accepted: 26 October 2023

Published online: 09 November 2023

© The Author(s) 2023 

Abstract

Collagen is a material which is recognized for its biocompatibility properties, biodegradability and low antigenicity, allowing it to be used for the creation of different materials as composites, scaffolds or hydrogels. However, collagen-based materials fail to provide useful mechanical properties in a final product. In this regard, it has been reported that the addition of metallic ions contributes towards supporting polymer matrices. Thus, the objective of this work was to evaluate the effect of metallic ions incorporation on the mechanical properties of biomaterials based on collagen from *Pterygoplichthys pardalis* and sodium polyacrylate (PAAS). It was observed that the addition of metallic ions modified the mechanical properties of biomaterials out of collagen and sodium polyacrylate (Co-PAAS). The greatest tensile force was achieved when 0.09 mg of collagen and 0.003 mol of Fe^{3+}/g Co-PAAS were used. On the other hand, the greatest elongation at break was achieved when the biomaterial was synthesized with 0.09 mg of collagen and 0.002 mol of K^{1+}/g Co-PAAS. Also, the highest value for Young's modulus was found when the biomaterial was synthesized with 0.05 mg of collagen and 0.002 mol of Fe^{3+}/g Co-PAAS and 0.003 mol of K^{1+}/g Co-PAAS. Finally, it was concluded that *P. pardalis* could be a collagen source for the development of biomaterials due to its electrostatic interactions with metallic ions increasing the mechanical properties of the processed material significantly.

Article highlights

- *Pterygoplichthys pardalis* is a tropical fish that could be used as collagen source to develop biomaterials.
- Collagen, sodium polyacrylate and ionic metals interact to generate a biomaterial with better mechanic properties.
- Ion Fe^{3+} generates materials with highest Young's modulus and tensile force.

Keywords Acid-soluble collagen (ASC) · Pepsin-soluble collagen (PSC) · Chelation · Scaffolding · Fish waste

JEL Classification L65

✉ Rocío Meza-Gordillo, rociomezagordillo@gmail.com; Amet Ovando-Roblero, amet_aorlive@live.com.mx; Daniel Castañeda-Valbuena, dacasval@gmail.com; José Humberto Castañón-González, jose.cg@tuxtla.tecnm.mx; Víctor Manuel Ruiz-Valdiviezo, victor.rv@tuxtla.tecnm.mx; Rodrigo Gutiérrez-Santiago, ibq.gutierrezsantiago@gmail.com; Alicia Grajales-Lagunes, grajales@uaslp.mx | ¹Chemical and Biochemical Engineering Department, Tecnológico Nacional de México/Instituto Tecnológico de Tuxtla Gutiérrez, Carretera Panamericana km 1080, C.P. 29050 Tuxtla Gutiérrez, Chiapas, Mexico. ²Faculty of Chemical Sciences, Universidad Autónoma de San Luis Potosí, Av. Dr. Manuel Nava No.6 - Zona Universitaria, C.P. 78210 San Luis Potosí, Mexico.



SN Applied Sciences

(2023) 5:321

| <https://doi.org/10.1007/s42452-023-05549-8>

SN Applied Sciences
A **SPRINGER NATURE** journal

1 Introduction

Collagen is the most abundant protein in vertebrate organisms, since it is distributed in different organs and tissues such as skin, bones, connective tissues, tendons, as well as in the extracellular matrix, where it provides flexibility, structural functions, and stability [1]. Currently, 29 types of collagens (I–XXIX) have been identified, each with different amino acid sequences, structure, and function [2]. However, all members of the collagen family have three polypeptide chains with a repetitive sequence of Gly-X-Y in their structure, where the X and Y positions usually are occupied by the amino acids proline and hydroxyproline. This sequence provides collagen a structural pattern in the form of a triple helix [3–5], which is different from other protein structures [6]. In addition, collagen has properties of biotechnological interest, such as high biocompatibility, biodegradability, and low antigenicity [7]. These are characteristics that have given the macromolecule a wide range of applications such as tissue engineering as a matrix than influences fibroblast contraction force, as a bio-inductive scaffold that supports human primary tendon-derived cell growth for articulation repair, as a high-strength, flexible, porous scaffold to promote tissue regeneration, and showed well-formed stratified epithelial layer, granulation tissue formation and collagen deposition [8–10].

Industrial marketed collagen is obtained from terrestrial organisms. However, there is a link between some collagen sources and viral diseases such as foot-and-mouth disease, transmissible spongiform encephalopathy, and avian influenza [11]. Thus, the extraction of collagen from fish has attracted the attention of researchers in the last decade [12, 13]. Furthermore, collagen that is recovered from aquatic species is a potential alternative and is considered as Generally Recognized As Safe (GRAS) by the Food and Drug Administration (FDA) [14]. The utilization of fish for collagen extraction must consider the diverse range of fish species, each with inherent variations in their collagen molecules, and the collagenous material is more prone to degradation because it contains lower amounts of crosslinks [15].

Recent studies have indicated that collagen from fresh water tropical species (tilapia) was more thermostable than the extracted from marine cold adapted fish (cod and hake). This has been related to the lower extent of proline regions and to a decreased proline hydroxylation degree of the collagen of cold-water marine fish [16]. Acharya et al. [17], reported that collagen extracted from silver carp relative solubility and thermal denaturation are more stable than milk shark owns to inter- and intra-molecular crosslinks and to a better structural

arrangement as seen in FT-IR spectra. Collagen extraction methods are traditionally based on the use of acidic solutions, which dissociate intermolecular cross-links of the aldimine type, causing swelling of fibrillar structures and denaturation [18]. However, enzymes (pepsin, trypsin, papain, etc.) are able to cleave peptides at telopeptide region and have become an alternative to traditional acidic collagen extraction methods [19].

Collagen promotes cell adhesion, growth, and differentiation; hence it is used for 2D, and 3D structures aimed at tissues and organs [20, 21]. However, the use of collagen as a single component produces materials with low mechanical strength that can be difficult to handle [7, 22]. For this reason, the addition of different materials is being used currently with the aim of improving its mechanical properties, as they interact with the collagen matrix [23]. Therefore, it is necessary to develop a variety of crosslinking methods, including chemical, physical, and biological methods, to alter the molecular structure of various natural polymers, further enhance the mechanical properties of collagen, and meet specific application requirements [24]. Hydroxyproline is a compound that is rich in hydroxyl groups, which tend to improve interaction capabilities and may contribute towards generating thermally stable polymeric complexes [25] if hydroxyl groups interact electrostatically with some added components. In this sense, metallic ions have great potential, as they promote electrostatic interactions, conferring greater stability in the final compound [26] that can improve if metallic ions interact with an anionic polyelectrolyte as sodium polyacrylate (PAAS). The addition of this component increase properties significantly, such as greater tensile stress [27] and elastic modulus [28, 29]. Besides, the addition of ions such as zinc, calcium, copper and iron generates polymeric materials with probable biological properties as wound repair [30].

The devilfish (*Pterygoplichthys pardalis*), also known as pleco, is a type of tropical catfish that has proven to be invasive and destructive [31]. It was introduced in various countries as an ornamental fish, which then caused the affectation of local ecosystems [32]. This species is one of the greatest threats to biodiversity in inland aquatic ecosystems due to its negative effects [33, 34]. *Pterygoplichthys pardalis* being a tropical fish, it is expected that the content of hydroxyproline in collagen is important and probably increase the interactions with metallic ions, contributing to the generation of durable polymer. Therefore, the objective of this work was to study the effect of metallic ion incorporation on the mechanical properties of biomaterials based on tropical fish-derived collagen from *Pterygoplichthys pardalis* and sodium polyacrylate (PAAS).

2 Materials and methods

2.1 Source of raw materials

Fish samples were obtained from the Peñitas dam, located in the Municipality of Tecpatán, Chiapas, Mexico, and were transported in coolers at 6 °C. The skins were manually separated in the laboratory and then dried at a temperature of 50 °C.

2.2 Pretreatment

The dried skins were ground in two stages. The first stage involved using a jaw crusher, and the second stage was carried out using a roller mill. Finally, the resulting flour was passed through a sieve with a 0.84 mm mesh and stored in polyethylene bags at 6 °C until it was used.

Next, 100 g of dry skin were mixed with 0.1 mol/L NaOH at a ratio of 1:10 (w/v) and left to react for 6 h at 4 °C. The NaOH solution was changed after 3 h to remove non-collagen proteins and skin pigments. After 6 h, the solution was filtered under vacuum and the samples were washed with distilled water until a neutral or slightly basic pH (7.8) was reached [35]. The samples were then degreased using a modified version of the method proposed by Roseline et al. [36]. To achieve this, the samples were mixed with 10% butanol at a ratio of 1:10 (w/v) for 24 h at 4 °C. Excess butanol was removed by washing the samples three times with distilled water and filtering them using a vacuum pump. Finally, the samples were stored in refrigeration at -18 °C until their subsequent use.

2.3 Collagen extraction

The extraction of acid-soluble collagen was carried out by mixing the pretreated samples with 0.5 M acetic acid for 72 h in a 1:15 ratio (w/v). Collagen was subsequently precipitated by adding 1.5 M NaCl and 0.05 M tris hydroxymethyl aminomethane (pH 7.0). The precipitated collagen was recovered by centrifugation for 50 min at 4500 rpm, after which the supernatant was discarded. The recovered collagen was dissolved in 100 mL of 0.5 M acetic acid and dialyzed with a 14 kDa pore size cellulose membrane (Sigma Aldrich) measuring 49 mm × 79 mm against 50 volumes of 0.1 M acetic acid for 24 h. The dialysis product was then filtered using Number 2 filter paper. Subsequently, a second dialysis process was carried out at 4 °C against 10 volumes of 0.1 M acetic acid. The distilled water solution was changed every 12 h until

a neutral pH was reached [34]. This extract was referred to as acid-soluble collagen (ASC).

For the collagen extraction by hydrolysis with pepsin, the pretreated samples were mixed with 0.75% pepsin (w/w) in 0.5 M acetic acid at a ratio of 1:15 (w/v) and stirred continuously for 72 h at 4 °C. The collagen was then precipitated by adding 1.5 M NaCl and tris hydroxymethyl aminomethane (pH 7.0). The precipitated collagen was recovered by centrifuging for 50 min at 4500 rpm, and the supernatant was discarded. The recovered collagen was dissolved in 100 mL of 0.5 M acetic acid and dialyzed against 50 volumes of 0.1 M acetic acid for 24 h, using a 49 mm × 79 mm cellulose membrane (Sigma Aldrich) with a pore size of 14 kDa. The dialysis product was filtered using filter paper Number 2. Then, a second dialysis process was performed against 10 volumes of acetic acid 0.1 M at 4 °C. The distilled water solution was changed every 12 h until a neutral pH was reached [37]. This extract was named pepsin-soluble collagen (PSC). Finally, the collagen obtained from both the acid extraction and enzymatic extraction processes was freeze-dried at 0.520 mbar (Labconco, Kansas, USA) and stored at -18 °C until further use. The collagen with the highest extraction yield was selected for the subsequent elaboration of the materials.

The performance of acid-soluble collagen (ASC) and pepsin-soluble collagen (PSC) was calculated from the percentage of dry weight of the skin used initially.

2.4 Analyses

2.4.1 UV–VIS spectroscopy

The ASC and PSC samples were dissolved in 0.5 M acetic acid at a concentration of 1 M, and a spectral scan from 200 to 800 nm was performed to identify the maximum absorbance wavelength using a UV–VIS spectrophotometer model DR 5000 (HACH, Colorado, USA) [38]. The quantification of protein content was performed using Lowry's method. Bovine serum albumin (BSA) was used as a standard to prepare the standard curve, while 0.5 M acetic acid was used for the negative control. The positive control sample used was collagen type I from Sigma Aldrich (Mexico).

2.4.2 Fourier transform infrared spectroscopy

The spectra were recorded using lyophilized collagen on a Nicolet™ IR spectrophotometer (Thermo Scientific, Massachusetts, USA). The spectra were scanned 16 times and measured in the range of 1000–4000 cm⁻¹ with a resolution of 4 cm⁻¹. The sample was directly placed on the FTIR spectrometer with an Agilent diamond ATR sample.

The control sample used was type I collagen from Sigma Aldrich.

2.4.3 Nuclear magnetic resonance (¹H-NMR)

The nuclear magnetic resonance spectra were recorded using an Agilent 500 MHz DD2 spectrometer (California, USA). The experiments were conducted at 25 °C, with the solvent signal (deuterated HCl) carefully chosen to avoid interference with any signal. Following dissolution, approximately 1 mL of the collagen sample solution was transferred to a 5 mm MRI tube and inserted into the magnet. After allowing 10 min for thermal equilibrium, the experiment was performed. The control sample used was collagen type I from Sigma Aldrich.

2.4.4 SDS-PAGE electrophoresis

The electrophoretic patterns were obtained through electrophoresis in a polyacrylamide gel with sodium dodecyl sulfate (SDS-PAGE), using the method of Laemmli [39] with slight modifications. A mini-protein vertical electrophoresis system (Bio-Rad, USA) was employed. A solution of ASC and PSC at a concentration of 1 M in 0.05 M acetic acid was prepared. Subsequently, a mixture was made by adding Laemmli sample buffer in a 1:1 ratio, which contained 12.48% Tris-HCl (pH 6.8), 6% (w/v) SDS, 12.52% (v/v) glycerol, 14.96% (v/v) mercaptoethanol, and 3 g bromophenol. The samples were heated at 90 °C for 5 min and allowed to cool to room temperature. For electrophoresis, a 7.5% separation gel and a 4% stacking gel were utilized. Subsequently, 10 µL of the solution from each sample were deposited in each of the gel wells, along with 10 µL of molecular marker and 10 µL of standard type I collagen (Sigma Aldrich). Electrophoresis was conducted at 100 V for 70 min, using 1X run buffer (Tris/Glycine/SDS) [40]. After the electrophoresis, the protein bands were stained with a solution of 0.1% Coomassie R-250 blue dissolved in water, methanol, and acetic acid (13:5:2, v/v/v) for 6 h. Then, the bands were destained using a solution of water, methanol, and acetic acid (13:5:2, v/v/v) [11]. The positive control used was collagen type I (Sigma Aldrich).

2.4.5 Intrinsic viscosity

The collagen isolated from devilfish was dissolved in concentrations ranging from 0.1 to 0.5 M in 0.5 M acetic acid. A negative control consisting of only 0.5 M acetic acid was also prepared. The viscosity of each solution was measured using an SVM 3000[®] viscometer (Anton Paar, Graz, Austria). The intrinsic viscosity of collagen was calculated using the Kuhn-Mark-Houwink-Sakurada equation based

on the dynamic viscosity measurements [41]. The positive control used in the experiment was collagen type I.

$$[\eta] = KM^\alpha \quad (1)$$

where η is the intrinsic viscosity, M is the mean molecular weight, K and α are specific values for proteins (1.86×10^{-19} and 1.8 for collagen, respectively).

2.4.6 Amino acid analyses

A Hitachi L-8900 amino acid analyzer (NY, USA) equipped with a 4.6 mm ID \times 60 mm ion-exchanged resin-packed column was used for analysis. To prepare the sample, 0.2 mg of the sample was suspended in 800 µL of performic acid (PA) and left overnight under a nitrogen atmosphere at 55 °C. After drying, the sample was hydrolyzed by adding 200 µL of 4.2 N NaOH at 110 °C for 24 h. To neutralize the hydrolysate, 200 µL of 4.2 N HCl and 600 µL of Nle diluent were added. A second hydrolysis was performed in the liquid phase by using 200 mL of a 6N HCl/1% phenol solution at 110 °C for 24 h. The resulting hydrolysate was dried under a nitrogen atmosphere at 55 °C and then adjusted to 1 mL with the Nle dilution buffer. The sample was vigorously stirred, and an aliquot of 50 µL was used for analysis. Nle's solution was used as an internal standard [42].

2.4.7 Elaboration of chelated materials (Col-PAAS-Metal)

Collagen solutions were prepared with 0.5 M acetic acid at different concentrations (0.005, 0.007, and 0.009 M of PSC). In parallel, metallic salt solutions were prepared (KCl, CaCl₂, and FeCl₃) at concentrations of 0.001, 0.002, and 0.003 mol/g of dry Collagen-Polyacrylate (Col-PAAS). A mixture of 40 mL of the metallic salt solutions, 10 mL of the PSC solution, and 40 mL of a 6.25% w/v sodium polyacrylate solution (Sigma Aldrich, Mw: 94.04 g/mol) was prepared at room temperature with mild mechanical stirring [29]. The mixture was then poured into rectangular silicone molds (6.6 cm \times 3.81 cm \times 2.54 cm) and left to dry in the extraction hood for 4 days. Finally, the biomaterial was conditioned by placing it in a desiccator with a saturated solution of sodium chloride (25 \pm 0.5 °C, 70 \pm 5% RH).

2.4.8 UV-Vis spectroscopy of the biomaterial-forming solution

For determining the maximum absorbance wavelength of the chelated polymer in the materials, a PSC solution (10 mL) was added at a concentration of 0.009 M in 0.05 M acetic acid. Subsequently, solutions of metallic salts (FeCl₃, CaCl₂, KCl) were added (40 mL) at a concentration

of 0.003 mol/g dry mass Col-PAAS, along with 40 mL of a 6.25% w/v sodium polyacrylate solution. The determination of the maximum absorbance wavelength was performed using a DR 5000 UV–VIS spectrophotometer (HACH, Colorado, USA), by performing a spectral scan of 200–800 nm [43]. The control sample consisted of a collagen solution at a concentration of 0.009 M with PAAS and sodium polyacrylate at 6.25% w/v, without any added metallic ions.

2.4.9 Determination of mechanical properties

The tensile stress, elongation at break, and Young's modulus of the materials were determined using the method developed by Xiao et al. [44], with modifications. An XT PLUS texture analyzer (Stable Micro Systems, Godalming, UK) was used for this purpose. Rectangular-shaped sheets, 5 cm × 1 cm (length × width), were cut from the samples for analysis, and the results were the average of three measurements. The crosshead speed was set at 0.3 mm/s with an initial distance of 30 mm until the samples broke. The tensile stress and elongation at break were calculated using the following equations.

$$\sigma = \frac{F}{A_0} \quad (2)$$

$$e = \frac{L - L_0}{L_0} \times 100 \quad (3)$$

$$\sigma e = E.e \quad (4)$$

where σe is tensile stress (MPa), F is the maximum force (N), A_0 is the initial section (mm^2), e is elongation or unit deformation (%), and L (mm) is the width of the test specimen, respectively. Finally, L_0 (mm) is the initial length of the test specimen and E is Young's modulus (MPa). The negative control was the material made of collagen solution at a concentration of 0.009 mg mL⁻¹ with PAAS at 6.25% w/v without metal ions.

2.4.10 Infrared spectroscopy (FT-IR) of chelated biomaterials

The spectra of the materials synthesized from collagen-PAAS-metal ions were recorded using a Nicolet™ IR spectrophotometer model (Thermo Scientific, Massachusetts, USA). Spectra were scanned 16 times and measured at 400–4000 cm⁻¹ with a resolution of 4 cm⁻¹ [45]. For each sample, the material was placed directly on the FTIR spectrometer fitted with an Agilent diamond ATR sample. The positive control was the material obtained from collagen

solution at a concentration of 0.009 mg mL⁻¹ with PAAS and sodium polyacrylate at 6.25% w/v without metal ions.

3 Results

3.1 Collagen extraction

Acid-soluble collagen and pepsin-soluble collagen were isolated from the skin of *Pterygoplichthys pardalis*, yielding 0.30 ± 0.08% and 4.46 ± 0.10% of dry weight (DW), respectively. These results are consistent with the reported yields for the extraction of collagen from the skin of striped catfish (*Pangasianodon hypophthalmus*), where the yields of ASC and PSC were 5.1% and 7.7%, respectively [46].

The treatment with pepsin generated higher yields than the method using acid, as reported in studies on catfish (ASC, 16.80%; PSC, 28%) [2] and paddlefish (ASC, 53%; PSC, 66%) [47]. This suggests that a large amount of collagen from the devilfish's dermal plates was cross-linked through covalent bonds via condensation of aldehyde groups in the telopeptide region, as well as by intermolecular cross-linking. These cross-links hinder the solubilization of collagen in an acidic environment. In contrast, enzyme treatment generates higher yields compared to acid extraction, but the characteristics of the extracted collagen, such as the size of the molecules and the distribution of molecular weight, depend mainly on the treatment time and the concentration of the enzyme. Pepsin affects the telopeptide region where collagen molecules are crosslinked, allowing extraction with greater performance and without damaging the integrity of the triple helix. The product resulting from hydrolysis is called atelocollagen, which results from the removal of terminal amino and carboxyl residues which act as antigens located on non-helical protein sections [17].

Because PSC presented the highest extraction performance, it was chosen for the elaboration of the materials and characterization.

3.2 UV–Vis spectroscopy

The maximum absorbance wavelengths observed for ASC and PSC were 240 and 236 nm, respectively (Fig. 1). The data obtained showed the presence of protein in extracts from both extraction methods, which was likely collagen. This matches with the results reported for collagen obtained from northern pike scales [48], skin from the Pacific cod [49], carp skin [3], and fish waste [50]. The UV absorption that was visualized in the spectrum was related to the –COOH, CONH₂ groups present in polypeptide chains, as well as to the n → π* electron transition of C=O in the peptide bond [51]. Approximately, proteins show

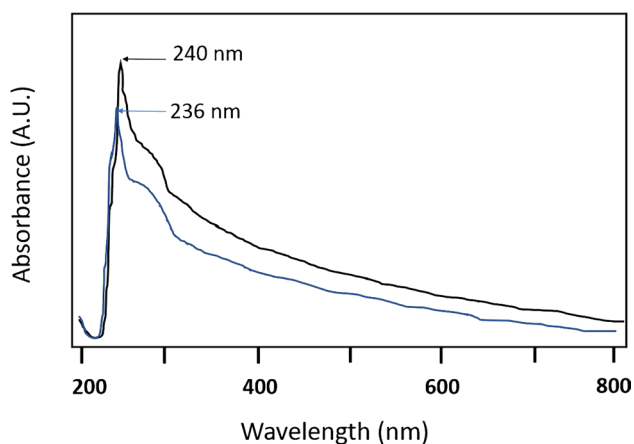


Fig. 1 UV–VIS spectra of collagen extracted from *Pterygoplichthys pardalis* skin by acid (ASC—black line) and pepsin (PSC—blue line) methods. The solvent used was HAc 0.5 M and the collagen concentration was the same in both solutions

Table 1 Composition of amino acids from pleco collagen (PSC)

Amino acids	Conc μM/mg	c/1000 resi- dues
Asp	0.19	52
Thr	0.1	27
Ser	0.16	44
Glu	0.27	74
Pro	0.4	110
Gly	1.16	319
Ala	0.43	118
Val	0.1	27
Ile	0.06	16
Leu	0.08	22
Tyr	0.02	5
Phe	0.04	11
His	0.03	8
Lys	0.1	27
Arg	0.19	52
Hyl	0.02	5
Hyp	0.22	60
Cys	0.02	5
Met	0.05	14
Trp	0.003	1

maximum absorbance at 280 nm, because of the influence exerted by some of the amino acid side chain bonds such as phenylalanine, tyrosine, tryptophan [34]. The wavelength value obtained for collagen extracted from devilfish skin was lower than that of other proteins. This could be since collagen obtained from *P. pardalis* skin is lacking in tyrosine and phenylalanine, which are sensitive chromophores that contribute to ultraviolet absorption at 280 nm

[3, 5]. In addition, it has a relatively high abundance of glycine and proline (Table 1).

3.3 Fourier transform infrared spectroscopy

The spectral analysis using FTIR showed the characteristic signals of amides A and B, as well as amides I, II, III (as seen in Fig. 2). The main signals in the collagen spectra were like the signals of collagen from other fish species and aquatic organisms, such as softshell turtle [52], pufferfish skin [53], milkfish and silver carp [54, 55].

The amide A band for ASC was found at 3277 cm^{-1} and 3291 cm^{-1} for PSC, which is associated with N–H stretching vibrations. Such vibrations occur in the range of $3400\text{--}3440\text{ cm}^{-1}$, which are assigned to the stretching mode and help demonstrate that the NH groups in both types of extracted collagens are related to hydrogen bonds, probably with a carbonyl group from the peptide chain. Amide B bands were found at 2921 cm^{-1} for ASC and 2924 cm^{-1} for PSC, which are associated with an asymmetric chain of the CH_2 group [56]. Amide I, bands II and III are known to be responsible for the degree of molecular order found in collagen, as well as participating in the formation of the triple helix structure resulting from CO stretching, N–H bending and C–H stretching, respectively. Amide bands I, II and III were found at 1635 , 1550 , and 1240 cm^{-1} for ASC and 1641 , 1545 , and 1241 cm^{-1} for PSC, respectively. According to Peng Sun et al. [25], if the result of dividing the value for the amide III band over the band corresponding to the displacement of $1450\text{--}1454\text{ cm}^{-1}$ is approximately 1, this indicates that the triple helical structure is intact. For the spectra of (ASC) and (PSC), ratios of 1.17 were obtained, suggesting that triple helix structure was intact [51].

3.4 Nuclear magnetic resonance ($^1\text{H-NMR}$)

The presence of a triple helix structure in collagen can be elucidated through $^1\text{H-NMR}$ spectroscopy. The formation of a triple helix structure results in the appearance of a new set of chemical shifts, which cannot be observed in the structure of denatured or non-assembled collagen.

The resonance spectra for both ASC and PSC samples shows the characteristic resonances of collagen-like triple-helices. The $\text{Pro C}^{\text{d}}\text{H}_{\text{1,h}}$ signals at 3.55 and 3.10 ppm and the $\text{Hyp C}^{\text{b}}\text{H}_1$ resonance at 2.08 ppm, confirm the triple helical structure [57, 58] (Fig. 3). Chemical displacements at 1.23 ppm indicate an acidic reaction between proline and tryptophan [59].

NMR analysis confirmed the presence of water molecules in both ASC and PSC, corresponding to the chemical displacement of the singlet at about 4.6–4.8 ppm [60, 61]. The intense band observed at 4.8 ppm indicated

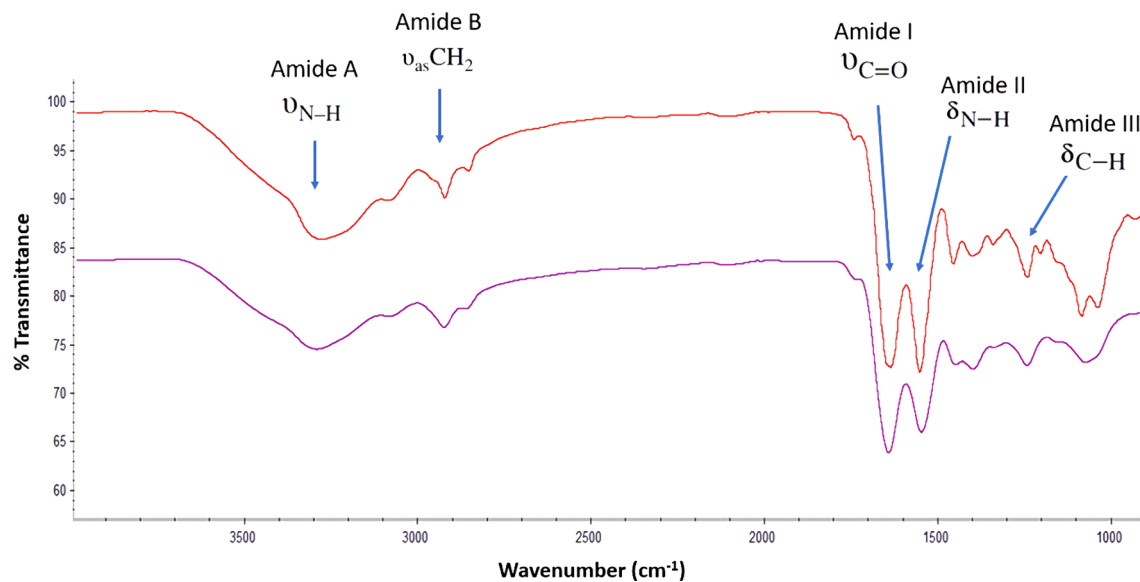


Fig. 2 FTIR spectra of collagen extracted from *Pterygoplichthys pardalis* skin by acid (ASC—red line) and pepsin (PSC—purple line) methods. IR spectra show the typical corresponding bands of col-

lagen: ν indicates the stretching vibration, ν_{as} indicates the stretching asymmetric vibration, and δ indicates the bending vibrations

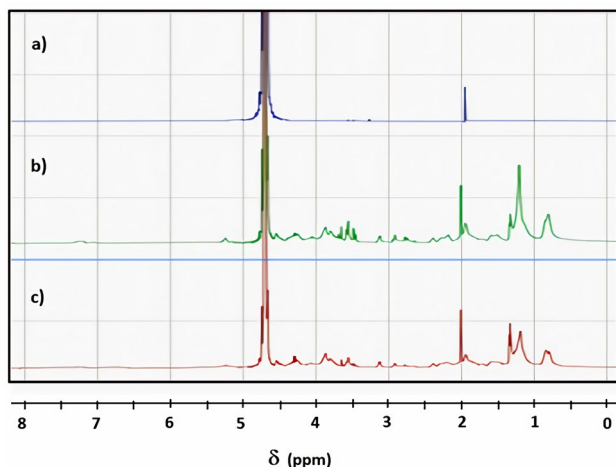


Fig. 3. $^1\text{H-NMR}$ spectra for **a** type 1 collagen standard, collagen extracted *Pterygoplichthys pardalis* skin by using **b** the pepsin method (PSC) and **c** the acid method (ASC). PSC and ASC spectra exhibit similarities between them, and the differences observed compared to the collagen could be due to impurities

the presence of hydration water, which constitutes about 0.5 g of water/g of collagen. This fraction of water includes the bound water interacting with the collagen's surface, along with the "structural" water that stabilizes the collagen helix [62].

3.5 SDS-PAGE electrophoresis

SDS-PAGE data from collagen samples are shown in Fig. 4. It is noteworthy that the band patterns in both ASC and PSC allow two different α chains to be identified, α_1 and α_2 , with a molecular size of 139 and 128 kDa, respectively [5]. Presence of a β chain dimer with a molecular size of 195 kDa was also observed. [63]. Also, the γ chain trimer formed by intramolecular and intermolecular crosslinking of the three chains was detected [64].

Type I collagen is composed of 2 identical α_1 subunits and one α_2 subunit, according to studies by Felician et al. [65], Salvatore et al. [6], and Peng Sun et al. [25]. Type I collagen is the primary collagen found in fish skin and scales, as reported in various studies. The band patterns identified in this analysis are consistent with findings reporting type I collagen in silver carp (α_1 with MW less than 120 kDa; α_2 , with MW less than 115 kDa) [66] and yellowfin tuna (α_1 with MW less than 120 kDa; α_2 with MW less than 150 kDa) [67]. The presence of β and γ chains indicates the presence of the dimer and trimer, respectively, suggesting that the extraction process and the addition of pepsin did not affect the native structure of collagen [68].

3.6 Measurement of viscosity and molecular weight

The intrinsic viscosity is a parameter that reflects the hydrodynamic volume occupied by macromolecules in solution and is related to their molecular weight [69]. The intrinsic viscosity values obtained for ASC and PSC were

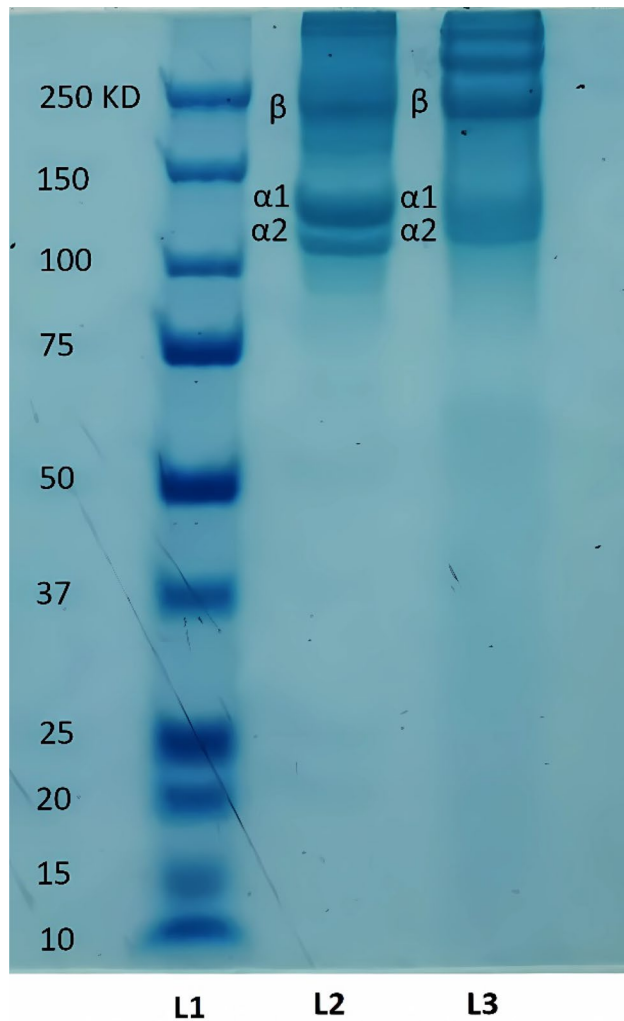


Fig. 4 SDS-PAGE performed on collagen samples under denaturing conditions. Line 1 (L1) represents the high molecular weight marker. Line 2 (L2) refers to the collagen extracted by pepsin method (PSC), and the line 3 (L3) refers to the collagen extracted by acid method (ASC). Collagen extracted from *Pterygoplichthys pardalis* skin with both methods, PSC and ASC, exhibit the presence of $\alpha 1$, $\alpha 2$, and β bands, typical of the type 1 collagen

23.81 and 13.66 dL/g, respectively. By using the Kuhn-Mark-Houwink-Sakurada equation, the average molecular weight was estimated to be 412 and 302 kDa for ASC and PSC, respectively. A standard collagen molecule usually has a size of 300 kDa, which corresponds to 100 kDa for each of the alpha strands [70]. A molecular weight higher than 300 kDa indicates the presence of cross-linking between collagen molecules and therefore suggests the formation of dimers and trimers [71]. These results indicate that ASC and PSC collagen types obtained in this study retained their native triple helix structure [49] (Fig. 5). Thus, the viscosity measurements suggest that collagen molecules from devilfish are likely cross-linked by covalent

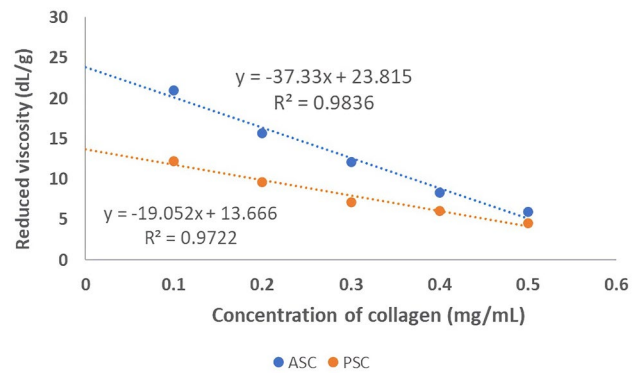


Fig. 5 Reduction of the intrinsic viscosity as function of collagen concentration. It demonstrates that at higher concentrations of collagen, the reduced viscosity is lower in both cases. Furthermore, the intrinsic viscosity obtained for collagen extracted using the acid method (ASC) is higher than that obtained to collagen extracted using the pepsin method (PSC)

bonds that occur via condensation of aldehyde groups in the telopeptide region and intermolecular cross-links, which ultimately reduces collagen solubility [72].

3.7 Amino acid analyses

Table 1 shows the amino acid composition of *P. pardalis* skin collagen. Pepsin produced a higher collagen yield, so the subsequent analyses were exclusively carried out with PSC. Collagen from this fraction had relatively high levels of glycine (29.8%), as well as alanine, glutamic acid, proline, and hydroxyproline. The structure of collagen is based on a repetitive sequence of $(\text{Gly-Pro-Hyp})_n$, where glycine represents almost one-third of the total residues. This amino acid is crucial for the formation of the triple helix, as it allows for the union of α chains through its side chain R. This, in turn, enables the formation of long and stable structures. Any other amino acid would prevent the binding of α chains [73].

Proline and hydroxyproline are important amino acids in collagen due to the presence of pyrrolidine rings, which restrict the conformation of the polypeptide chain and stabilize the collagen triple helix [2]. In this study, proline was the third most abundant amino acid, representing approximately 10% of the total amino acids in collagen. Hydroxyproline was the fifth most abundant amino acid, accounting for 6% of the total. However, hydroxylysine was not significant, representing only about 0.5% of the total. Interestingly, collagen derived from species living in cold environments has lower levels of amino acids containing imine fractions, such as proline and hydroxyproline, compared to terrestrial organisms. This is likely due to the evolutionary adaptation of aquatic organisms to lower body temperatures, resulting

in collagen with a lower melting point and thermal stability, and lower concentrations of these amino acids [74].

The absence of cysteine in the obtained collagen underscores the presence of type I collagen. Generally, type I collagen has a low cysteine content, typically around 0.2%, and a methionine content ranging from 1.24 to 1.33% [75]. The use of pepsin during the extraction method may also influence these contents by reducing the percentages of Tyr and His, which are present in lower quantities in PSC. This protease affects the bond between Tyr and His, resulting in lower levels of these two amino acids [54]. These findings are consistent with those obtained for other aquatic species, such as *Rhopilema esculentum* [76], *Takifugu flavidus* [77], *Scomber japonicus* [78].

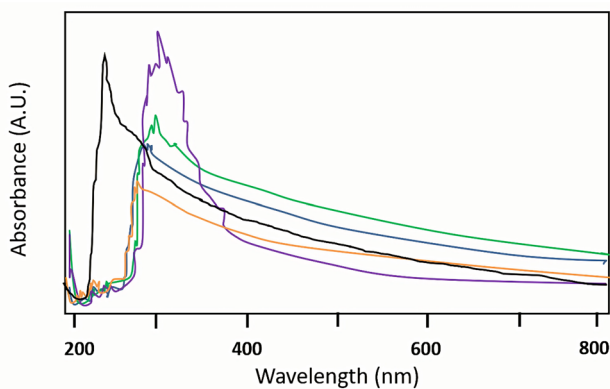


Fig. 6 UV–VIS spectra of collagen extracted from *Pterygoplichthys pardalis* skin by acid (ASC—black line), control (Col-PAAS—orange) and biomaterials based on collagen chelated with various metal ions: potassium (blue), calcium (green) and iron (purple). The graph demonstrates the effect of adding PAAS and metals on collagen, highlighting the interaction between the different components of the mixture

3.8 UV–VIS spectroscopy for biomaterial-forming solution

The material composed of collagen and sodium polyacrylate (control) exhibited a λ max of 302 nm, which was 66 nm higher than that of pure collagen. This can be attributed to the polyanionic structure of sodium polyacrylate, which can absorb light and form electrostatic interactions with positively charged species such as alginates, proteins, and metal ions [79]. On the other hand, the λ max for the Col-PAAS-K complex was identified at 314 nm, which was 12 nm higher than the control made with the biomaterial formulated with collagen and sodium polyacrylate (Col-PAAS). In the case of the Col-PAAS-Ca complex, the λ max was identified at 322 nm, which was 20 nm higher than the control. Finally, for the Col-PAAS-Fe complex, the λ max was found at 326 nm, which was 24 nm higher than for the control (Fig. 6). These findings indicate that an interaction exists among the components of the biomaterial. The shift in the maximum absorbance wavelength when adding the different metal ions may be due to structural changes in carbonyl oxygen during chelation [80]. These changes in the intensity of the absorption band or wave suggest that the peptide may be forming new complexes by bonding with metals at metallic binding sites [43, 80].

Once the solutions were formulated the biomaterials were prepared according to the methodology previously described. The materials chelated with various metal ions are shown in Fig. 7.

4 Mechanical properties of chelated biomaterials

The concentration of collagen (ranging from 0.005 to 0.009 mg mL⁻¹) affects the tensile stress, elongation at break, and Young's modulus of the materials (Fig. 8). This is because the increased concentration of collagen leads to

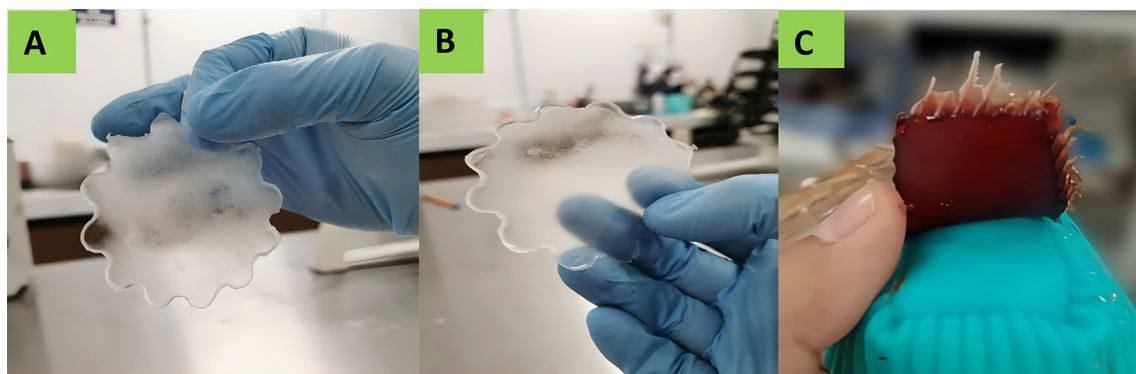


Fig. 7 Material formed with collagen extracted from *Pterygoplichthys pardalis* skin, CO-PAAS chelated with K⁺ (A), Ca²⁺ (B), and Fe³⁺ (C)

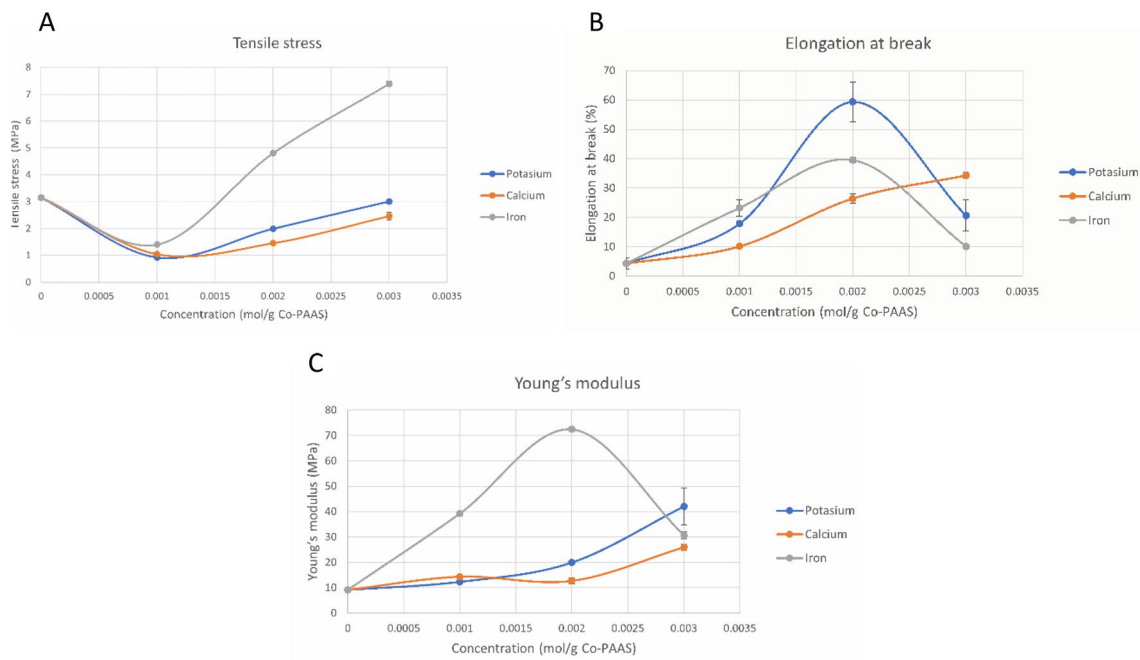


Fig. 8 Diagrams of **A** Tensile stress, **B** Elongation at break, and **C** Young's modulus for materials with different metallic ions

the formation of denser structures [81]. Collagen's unique amino acid sequence, including glutamic acid, aspartic acid, arginine, and lysine, provides a greater number of binding sites and is capable of electrostatic interactions with metal ions [82, 83].

The addition of metal ions to Col-PAAS materials increased structural stability due to metal coordination by multiple triple helices. Metal ions can interact with functional groups, and strong metal–ligand interactions can remodel flexible regions of the protein to adopt a metal coordination site at the collagen's terminal chains, leading to increased cross-linking and resulting in superior structures [84]. It was demonstrated that

the mechanical stability provided by the metal ions depended on their valence state.

Table 2 shows the effect of metallic ion concentration on the mechanical properties of the biomaterial. The treatment that yielded the best results ($P < 0.05$) in terms of tensile strength was the one that included iron at concentrations of 0.002 and 0.003 mol/g Col-PAAS, resulting in values of 4.80 and 7.38 MPa, respectively. In contrast, the inclusion of K^+ and Ca^{2+} ions did not improve this mechanical variable, as the negative control (Col-PAAS) had a higher value of 3.15 MPa than any of the concentrations of these two metal ions.

Table 2 Tensile stress (MPa), elongation at break (%) and Young's modulus for Co-PAAS biomaterials with different metallic ion concentrations: K^+ , Ca^{2+} and Fe^{3+}

Samples	Concentration mol/g Co-PAAS	Tensile stress (MPa)	Elongation at break (%)	Young's modulus (MPa)
Co-PAAS	0	3.2 ± 0.1 ^c	4.3 ± 2.0 ^e	9.1 ± 0.4 ⁱ
Co-PAAS- K^+	0.001	0.9 ± 0.0 ^h	17.9 ± 0.9 ^d	12.3 ± 0.3 ^h
	0.002	2.0 ± 0.0 ^f	59.4 ± 6.8 ^a	20.0 ± 0.2 ^f
	0.003	3.0 ± 0.0 ^d	20.7 ± 5.3 ^{cd}	42.1 ± 7.3 ^b
Co-PAAS- Ca^{2+}	0.001	1.0 ± 0.1 ^h	10.2 ± 0.1 ^e	14.3 ± 0.6 ^g
	0.002	1.5 ± 0.0 ^g	26.4 ± 1.7 ^c	12.7 ± 1.2 ^e
	0.003	2.5 ± 0.1 ^e	34.3 ± 1.0 ^b	26.0 ± 1.2 ^d
Co-PAAS- Fe^{3+}	0.001	1.4 ± 0.1 ^g	23.3 ± 2.8 ^{cd}	39.3 ± 0.4 ^b
	0.002	4.8 ± 0.0 ^b	39.5 ± 0.8 ^b	72.5 ± 0.8 ^a
	0.003	7.4 ± 0.1 ^a	10.1 ± 0.7 ^e	30.7 ± 1.4 ^c

The increase in stress force is dependent on the concentration of the metallic ion, as the mechanical properties of biomaterials are related to the electrostatic interactions of the anionic carboxyl groups, as well as intra- and intermolecular interactions [29]. The chelation that occurs between collagen molecules and metallic ions increases the degree of cross-linking of the fibrils, generating a more compacted structure [80, 81, 85].

The elongation at break was found to be dependent on the concentration of metallic ions in the biomaterial. The treatment with the best results for elongation at break ($P < 0.05$) was the one that included potassium ions at a concentration of 0.002 mol/g Col-PAAS, which resulted in a 59.353% increase in the dimension of the material before breaking. The highest concentration of calcium ions (0.003 mol/g Dry Col-PAAS) caused an elongation before rupturing of 34.259%, while the lowest concentration of iron ions (0.001 mol/g Dry Col-PAAS) caused an elongation before maximum rupture of 23.254%. According to Ling et al. [86], the addition of divalent metallic ions such as Ni, Mg, and Co can increase the mechanical strength and significantly increase the elastic modulus of materials, compared to trivalent metal ions which significantly reduce breaking deformation. This phenomenon occurs because trivalent metallic ions can strongly bind to negatively charged groups (COOH and OH) in materials, providing highly cross-linked structures that make them less water-like and more solid [87]. The difference in mechanical properties between divalent and trivalent ions is attributed to the valence effect, where a higher valence leads to a more polarized ion cloud and, consequently, stronger attraction [84]. A slightly smaller radius results in excellent stability and the highest coordination strength in the Co-PAAS material system, causing materials chelated with Fe to be mechanically stronger compared to Ca and K [88].

The best results ($P < 0.05$) for Young's modulus were obtained with a concentration of 0.002 mol Fe^{3+} /g Col-PAAS, followed by 0.003 mol K^{+} /g Col-PAAS and, finally, with 0.001 mol Fe^{3+} /g Col-PAAS. Therefore, the addition of metallic ions increased Young's modulus of the materials. It was observed that a concentration of 0.003 mol Fe^{3+} /g Col-PAAS did not cause a greater increase in Young's modulus, a phenomenon that is due to the fact that the chelation between collagen and the iron ion saturated all sites corresponding to the functional groups of collagen and PAAS. That is, all of the binding sites corresponding to the functional groups of collagen had electrostatic interactions, and therefore, by adding a higher concentration of the iron ion, the mechanical variables were no longer favored [89]. This saturation phenomenon was not evidenced with the concentrations of calcium and potassium that were used, as the materials made when using these metals increased Young's modulus significantly as the concentration of the

ions increased. Therefore, the higher valence in Fe^{3+} and lower valences in K^{+} and Ca^{2+} cause the final materials to exhibit a different behavior both in tensile stress, elongation at break and Young's modulus, which will vary by increasing the concentration of the metals. Interactions may change the spatial structure and binding strength of material components [90].

It was expected that the chelation between calcium ions and collagen would increase the mechanical properties of the collagen fibril, as calcium ions naturally chelate with collagen in tissues such as tendons, bones, and ligaments. Wang et al. [91] and Wei et al. [92] have shown that chelation of metallic ions, such as Fe^{3+} , with proteins can form metallopolymer structures with strong mechanical properties, as iron ions have a valence of three, which can bind to free electron pairs. However, an increase in iron concentration could cause the breakdown of the network between collagen and PAAS, weakening the electrostatic force and resulting in a decrease in tensile strength [29].

As reported by Ge et al. [28], the mechanical characteristics of gelatin hydrogels can be adjusted by using different metal ions, varying temperatures, and changing soaking durations. The addition of iron to materials made from gelatin and tannic acid (DC-GT/OTA/ Fe^{3+}) can withstand compression stress of up to 65 MPa with a compressive strain of over 99% and exhibits excellent resistance to fatigue under repetitive loads, resulting in better stress force properties compared to materials synthesized from gelatin and tannic acid alone (SC-GT/OTA), this is due to the metallic coordination of Fe^{3+} and the OH groups of OTA.

Additionally, hydrogels crosslinked with metal ions demonstrate enhanced antibacterial properties against *Escherichia coli* and *Staphylococcus aureus*. The antibacterial properties are desired attributes of collagen wound healings, making them potentially valuable for various biological applications under natural bodily conditions.

Similarly, the study conducted by Wang, et al. [27] demonstrated that the addition of different metal ions increased the compressive strength of the materials. Pure gelatin material had a compressive strength value of 0.04 MPa, while the addition of Cr^{3+} and Fe^{2+} increased this mechanical variable by 53% and 67%, respectively. In contrast, the addition of Fe^{3+} increased the compressive strength up to 11.81 MPa, which was 295 times more than pure gelatin material and represented a 90% increase in this mechanical variable.

In the study by Cunha et al. [93], where they report the development of a biomaterial using type I collagen, alginate, and CaSO_4 , it was observed that increasing the concentration of Ca^{2+} resulted in an increase in the Young's modulus. However, it did not have an effect on the morphology of fibroblasts encapsulated in the material,

nevertheless, the cells were still able to spread and contract the matrix which enhanced the upregulation of key mediators of inflammation such as IL-10 and COX-2. These findings suggest that by modulating the mechanical properties of a wound dressing biomaterial on the wound site, it could regulate the progression of wound healing.

4.1 Fourier transform infrared spectroscopy

The interactions between metallic ions, collagen and PAAS were analyzed using FTIR spectrophotometry. All spectra pertaining to Col-PAAS-K, Col-PAAS-Ca, and Col-PAAS-Fe materials showed characteristic absorption bands assigned to peptide bonds in collagen, which are related to the absorptions of amide A, amide B, amide I, amide II and amide III. However, they presented displacement variations, suggesting the existence of an interaction among components [27, 43].

The displacement of the amide A band for Col-PAAS was 3284 cm^{-1} , which could be attributed mainly to the stretching vibration of the NH group that is found in the collagen peptides, as well as to electrostatic interactions with the oxygen in the sodium polyacrylate's carboxyl group. After chelation, the frequency of displacement increased to 3364 , 3341 and 3359 cm^{-1} for Col-PASS-K, Col-PASS-Ca, and Col-PASS-Fe, respectively. The displacement of this band was due to the hydrogen binding and to the coordination of nitrogen with metals K, Ca, and Fe. Overall, the coordinated amino groups showed a significant increase with respect to NH stretching frequencies, and it

was verified that the NH group is involved in the formation of the new complex [94, 95]. In the case of Col-PAAS-Ca, the absorption band for the NH group was the one that showed a smaller displacement regarding Col-PAAS, indicating smaller interactions with calcium (Fig. 9).

The displacement of the amide I band for the Col-PAAS complex was 1647 cm^{-1} . The amide I band spectra for Col-PAAS-K, Col-PAAS-Ca, and Col-PAAS-Fe, which corresponded to the stretching vibrations for the CO group, shifted to higher wavenumbers, which were 1655 , 1692 and 1642 cm^{-1} , respectively. These shifts indicated the formation of new bonds between metallic ions and the CO groups of the protein. Chelation is generated because the oxygen in the carbonyl group has a pair of non-bonding free electrons that interact with the atoms of metallic ions with empty electron orbits [29, 96, 97].

The amide II band represents the symmetrical and asymmetrical bending vibrations of the NH bond [98]. This band presented greater displacement in the spectra pertaining to complexes Col-PAAS-K, Col-PAAS-Ca, and Col-PAAS-Fe, which serves as evidence of interactions between this group and metals [99]. The amide III band represents a combination of NC stretching vibrations and NH deformation of amide bonds. This band also represents the bending vibrations of CH_2 groups from the carbonated glycine chain and proline side chains [38], where a displacement to a higher wavenumber was observed, implying an existing interaction between these groups and metals. In addition, the chelates showed a new absorption band at 650 cm^{-1} that was non-existent in the peptide spectrum,

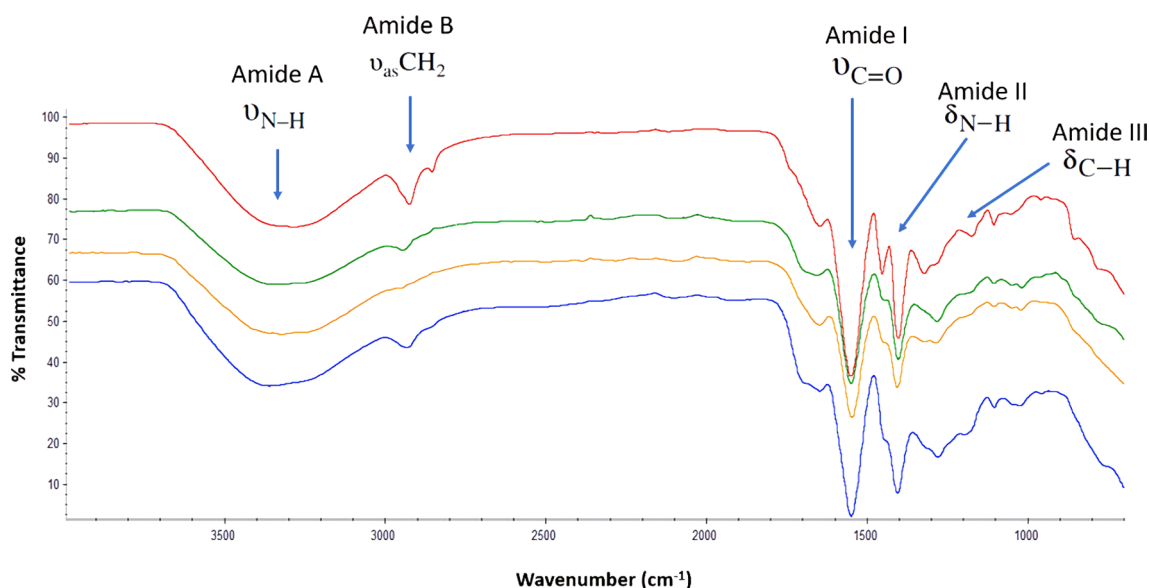


Fig. 9 FTIR spectra of the control corresponding to Col-PAAS (red) and collagen-based materials with different metal ions: potassium (green), calcium (yellow), iron (blue). ν indicates the stretching

vibration, ν_{as} indicates the asymmetric stretching vibration and δ indicates the bending vibration

which represents the coordination between the metallic ions and collagen [45].

In general, the FTIR spectra of Col-PAAS-K, Col-PAAS-Ca, and Col-PAAS-Fe showed differences compared to that of Col-PAAS, mainly in intensity and band displacement for the CN, CO, and NH groups. This suggests that these functional groups are involved in the formation of new complexes [100].

5 Conclusions

The Col-PAAS-K, Col-PAAS-Ca, and Col-PAAS-Fe matrices may improve the mechanical properties of tissue-engineered constructs. The incorporation of metal ions into the collagen matrix could enhance structural integrity, tensile strength, and overall stability, thereby providing superior support for tissue regeneration. The presence of K, Ca and Fe might exhibit improved biocompatibility, facilitating cell-material interactions, promoting favorable cellular responses and tissue integration.

Acknowledgements The authors are grateful to the National Science and Technology Council (México) (700741, R.G.S.; 957352, A.O.R. scholarships) and to Mexican National Technologic / Tuxtla Gutiérrez Technologic Institute for financial support (8848.20-P).

Data availability The authors declare that the data supporting the findings in this study are available in the manuscript figures and tables.

Declarations

Conflict of interest The authors declare that there are no conflicts of interest.

Open Access This article is licensed under a Creative Commons Attribution 4.0 International License, which permits use, sharing, adaptation, distribution and reproduction in any medium or format, as long as you give appropriate credit to the original author(s) and the source, provide a link to the Creative Commons licence, and indicate if changes were made. The images or other third party material in this article are included in the article's Creative Commons licence, unless indicated otherwise in a credit line to the material. If material is not included in the article's Creative Commons licence and your intended use is not permitted by statutory regulation or exceeds the permitted use, you will need to obtain permission directly from the copyright holder. To view a copy of this licence, visit <http://creativecommons.org/licenses/by/4.0/>.

References

1. Senadheera TRL, Dave D, Shahidi F (2020) Sea cucumber derived type I collagen: a comprehensive review. *Mar Drugs* 18:11–13. <https://doi.org/10.3390/md18090471>
2. Wang J, Pei X, Liu H, Zhou D (2018) Extraction and characterization of acid-soluble and pepsin-soluble collagen from

- skin of loach (*Misgurnus anguillicaudatus*). *Int J Biol Macromol* 106:544–550. <https://doi.org/10.1016/j.ijbiomac.2017.08.046>
3. Liu Y, Ma D, Wang Y, Qin W (2018) A comparative study of the properties and self-aggregation behavior of collagens from the scales and skin of grass carp (*Ctenopharyngodon idella*). *Int J Biol Macromol* 106:516–522. <https://doi.org/10.1016/j.ijbiomac.2017.08.044>
4. Lehnert S, Sikorski P (2021) Tailoring the assembly of collagen fibers in alginate microspheres. *Mater Sci Eng C* 121:111840. <https://doi.org/10.1016/j.msec.2020.111840>
5. Tung NQ, Trinh ND, Hoang T (2019) Characterization of collagen derived from tropical freshwater carp fish scale wastes and its amino acid sequence. *Nat Prod Commun*. <https://doi.org/10.1177/1934578X19866288>
6. Salvatore L, Gallo N, Natali Maria L, Campa L, Lunetti P, Marta M, Blasi Federica S, Corallo A, Capobianco L, Sannino A (2020) Marine collagen and its derivatives: versatile and sustainable bio-resources for healthcare. *J Neurol Sci* 113:116544. <https://doi.org/10.1016/j.jns.2019.116544>
7. Lohrasbi S, Mirzaei E, Karimizade A, Takallu S, Rezaei A (2020) Collagen/cellulose nanofiber hydrogel scaffold: physical, mechanical and cell biocompatibility properties. *Cellulose* 27:927–940. <https://doi.org/10.1007/s10570-019-02841-y>
8. Jin T, Li L, Siow R, Liu K (2016) Collagen matrix stiffness influences fibroblast contraction force. *Biomed Phys Eng Express* 2:047002
9. Heidar B, Mitchell C, Zheng M (2021) A bio-inductive collagen scaffold that supports human primary tendon-derived cell growth for rotator cuff repair. *J Orthopaedic Trans*. <https://doi.org/10.1016/j.jot.2021.10.00610>
10. Hayashi Y, Yamada S, Ikeda T, Koyama Z, and Yanagiguchi K (2012), Chitosan and fish collagen as biomaterials for regenerative medicine. In S.K. Kim, Ed. *Marine medical food*, vol. 65, chapter 6. Academic Press, London, pp 107–120
11. He X, Li W, Liu S, Li Y, Chen Y, Dan N, Dan W, Zhu M (2022) Fabrication of high-strength, flexible, porous collagen-based scaffolds to promote tissue regeneration. *Mater Today Biol*. <https://doi.org/10.1016/j.mtbio.2022.100376>
12. Tan Y, Chang SKC (2018) Isolation and characterization of collagen extracted from channel catfish (*Ictalurus punctatus*) skin. *Food Chem* 242:147–155. <https://doi.org/10.1016/j.foodchem.2017.09.013>
13. Chen S, Chen H, Xie Q, Hong B, Chen J, Hua F, Bai K, He J, Yi R, Wu H (2016) Rapid isolation of high purity pepsin-soluble type I collagen from scales of red drum fish (*Sciaenops ocellatus*). *Food Hydrocoll* 52:468–477. <https://doi.org/10.1016/j.foodhyd.2015.07.027>
14. Avila-Rodríguez MI, Rodríguez Barroso LG, Sánchez ML (2018) Collagen: a review on its sources and potential cosmetic applications. *J Cosmet Dermatol* 17:20–26. <https://doi.org/10.1111/jocd.12450>
15. Gómez-Guillén MC, Turnay J, Fernández-Díaz MD, Ulmo N, Lizarbe MA, Montero P (2002) Structural and physical properties of gelatin extracted from different marine species: a comparative study. *Food Hydrocoll* 16(1):25–34. [https://doi.org/10.1016/S0268-005X\(01\)00035-2](https://doi.org/10.1016/S0268-005X(01)00035-2)
16. Nurilmala M, Suryamarevita H, Husein Hizbullah H, Jacob AM, Ochiai Y (2022) Fish skin as a biomaterial for halal collagen and gelatin. *Saudi J Biol Sci* 29(2):1110. <https://doi.org/10.1016/j.sjbs.2021.09.056>
17. Acharya P, Kupendra M, Fasim A, More S, Murthy V (2022) A comparative assessment of collagen type 1 from silver carp (fresh water) and milk shark (marine) fish waste. *Biotech* 82(12):2190–2198. <https://doi.org/10.1007/s13205-022-03114-5>
18. Cozza N, Bonani W, Motta A, Migliaresi C (2016) Evaluation of alternative sources of collagen fractions from *Loligo vulgaris*

- squid mantle. *Int J Biol Macromol* 87:504–513. <https://doi.org/10.1016/j.ijbiomac.2016.03.013>
19. Ali A, Benjakul S, Prodpran T, Kishimura H (2018) Extraction and characterisation of collagen from the skin of golden carp (*Probarbus jullieni*), a processing by-product. *Waste Biomass Valor* 9:783–789. <https://doi.org/10.1007/s12649-017-9841-0>
 20. Castro-Piedra SE, Calvo-Castro LA, Alvarenga-Venutolo S, Centeno-Cerdas C, Ramos-Madrigal M, Vega-Baudrit J, Zamora-Mora V, Rojas-Chaves M (2015) Membranas de colágeno y quitosano de fuentes alternativas: evaluación para su uso potencial en ingeniería de tejidos. *Rev Tecnol en Marcha* 28:58. <https://doi.org/10.18845/tm.v28i5.2220>
 21. Park Y, Huh KM, Kang SW (2021) Applications of biomaterials in 3d cell culture and contributions of 3d cell culture to drug development and basic biomedical research. *Int J Mol Sci* 22:1–21. <https://doi.org/10.3390/ijms22052491>
 22. Kołodziejaska B, Kafak A, Kolmas J (2020) Biologically inspired collagen/apatite composite biomaterials for potential use in bone tissue regeneration—a review. *Materials* 13(7):1748. <https://doi.org/10.3390/ma13071748>
 23. Li Y, Liu Y, Li R, Bai H, Zhu Z, Zhu L, Zhu C, Che Z, Liu H, Wang J, Huang L (2021) Collagen-based biomaterials for bone tissue engineering. *Mater Des* 210:110049. <https://doi.org/10.1016/j.matdes.2021.110049>
 24. Parmar A, Xu F, Pike D, Belure S, Hasan N, Drzewiecki K, Shreiber D, Nanda V (2015) Metal stabilization of collagen and de novo designed mimetic peptides. *Biochem* 54:4987–4997. <https://doi.org/10.1021/acs.biochem.5b00502>
 25. Sun P, Ren Y, Wang S, Zhu H, Zhou J (2021) Characterization and film-forming properties of acid soluble collagens from different by-products of loach (*Misgurnus anguillicaudatus*). *Lwt* 149:111844. <https://doi.org/10.1016/j.lwt.2021.111844>
 26. Bhardwaj R, Kaur B, Singh JP, Kumar M, Lee HH, Kumar P, Meena RC, Asokan K, Hwa Chae K, Goyal N, Gautam S (2019) Role of low energy transition metal ions in interface formation in ZnO thin films and their effect on magnetic properties for spintronic applications. *Appl Surf Sci* 479:1021–1028. <https://doi.org/10.1016/j.apsusc.2019.02.107>
 27. Wang J, Fan X, Liu H, Tang K (2020) Self-assembly and metal ions-assisted one step fabrication of recoverable gelatin hydrogel with high mechanical strength. *Polym Technol Mater* 59:1899–1909. <https://doi.org/10.1080/25740881.2020.1773499>
 28. Ge S, Ji N, Cui S, Xie W, Li M, Li Y, Xiong L, Sun Q (2019) Coordination of covalent cross-linked gelatin hydrogels via oxidized tannic acid and ferric ions with strong mechanical properties. *J Agric Food Chem* 67:11489–11497. <https://doi.org/10.1021/acs.jafc.9b03947>
 29. Ma Y, Wang W, Wang Y, Guo Y, Duan S, Zhao K, Li S (2018) Metal ions increase mechanical strength and barrier properties of collagen-sodium polyacrylate composite films. *Int J Biol Macromol* 119:15–22. <https://doi.org/10.1016/j.ijbiomac.2018.07.092>
 30. Wang H, Xu Z, Li Q, Wu J (2021) Application of metal-based biomaterials in wound repair. *Eng Regen* 2:137–153. <https://doi.org/10.1016/j.engreg.2021.09.005>
 31. Lujan NK, Armbruster JW, Lovejoy NR, López-Fernández H (2015) Multilocus molecular phylogeny of the suckermouth armored catfishes (Siluriformes: Loricariidae) with a focus on subfamily Hypostominae. *Mol Phylogenet Evol* 82:269–288. <https://doi.org/10.1016/j.ympev.2014.08.020>
 32. Medellín-Castillo NA, Cruz-Briano SA, Leyva-Ramos R, Torres-Dosal A, Giraldo-Guti L, Moreno-Piraj JC, Labrada-Delgado GJ, Rodríguez-Estupi JP, Yobanny S, Lopez R, Selene M, Mendoza B (2020) Use of bone char prepared from an invasive species, pleco fish (*Pterygoplichthys* spp.), to remove fluoride and Cadmium (II) in water. *Environ Manag* 256:109956. <https://doi.org/10.1016/j.jenvman.2019.109956>
 33. Panase P, Uppapong S, Tunchareon S, Tanitson J, Soontornprasit K, Intawicha P (2018) Partial replacement of commercial fish meal with Amazon sailfin catfish *Pterygoplichthys pardalis* meal in diets for juvenile Mekong giant catfish *Pangasianodon gigas*. *Aquacult Rep* 12:25–29. <https://doi.org/10.1016/j.aqrep.2018.08.005>
 34. Nurubhasha R, Sampath Kumar NS, Thirumalasetti SK, Simhachalam G, Dirisala VR (2019) Extraction and characterization of collagen from the skin of *Pterygoplichthys pardalis* and its potential application in food industries. *Food Sci Biotechnol* 28:1811–1817. <https://doi.org/10.1007/s10068-019-00601-z>
 35. Abdollahi M, Rezaei M, Jafarpour A, Undeland I (2018) Sequential extraction of gel-forming proteins, collagen and collagen hydrolysate from gutted silver carp (*Hypophthalmichthys molitrix*), a biorefinery approach. *Food Chem* 242:568–578. <https://doi.org/10.1016/j.foodchem.2017.09.045>
 36. Roseline A, Pereira L, Mantelli M, Luis R, Aparecida I, Oliveira R, Mottin I, Cristina R, Dornelles P (2020) Extraction and characterization of collagen from sheep slaughter by-products. *Waste Manag* 102:838–846. <https://doi.org/10.1016/j.wasman.2019.12.004>
 37. Cumming MH, Hall B, Hofman K (2019) Isolation and characterisation of major and minor collagens from hyaline cartilage of hoki (*Macrurus novaezelandiae*). *Mar Drugs* 7:223
 38. Yuan B, Zhao C, Cheng C, Huang D, Cheng S, Cao C, Chen G (2019) A peptide-Fe(II) complex from *Grifola frondosa* protein hydrolysates and its immunomodulatory activity. *Food Biosci* 32:100459. <https://doi.org/10.1016/j.fbio.2019.100459>
 39. Laemmli UK (1970) Cleavage of structural proteins during the assembly of the head of bacteriophage T4. *Nature* 227:680–685. <https://doi.org/10.1038/227680a0>
 40. Sousa RO, Alves AL, Carvalho DN, Martins E, Oliveira C, Silva TH, Reis RL (2019) Acid and enzymatic extraction of collagen from Atlantic cod (*Gadus morhua*) swim bladders envisaging health-related applications. *J Biomater Sci Polym Ed* 31:20–37. <https://doi.org/10.1080/09205063.2019.1669313>
 41. Lewandowska K, Szulc M, Sionkowska A (2021) Effect of solvent on the hydrodynamic properties of collagen. *Polymers* 13(21):3626. <https://doi.org/10.3390/polym13213626>
 42. Zhao Y, Wang Z, Zhang J, Su T (2018) Extraction and characterization of collagen hydrolysates from the skin of *Rana chensinensis*. *Biotech* 8:1–8. <https://doi.org/10.1007/s13205-018-1198-y>
 43. Meng K, Chen L, Xia G, Shen X (2021) Effects of zinc sulfate and zinc lactate on the properties of tilapia (*Oreochromis niloticus*) skin collagen peptide chelate zinc. *Food Chem* 347:129043. <https://doi.org/10.1016/j.foodchem.2021.129043>
 44. Xiao J, Ma Y, Wang W, Zhang K, Tian X, Zhao K, Duan S, Li S, Guo Y (2021) Incorporation of gelatin improves toughness of collagen films with a homo-hierarchical structure. *Food Chem* 345:128802. <https://doi.org/10.1016/j.foodchem.2020.128802>
 45. Wu W, He L, Liang Y, Yue L, Peng W, Jin G, Ma M (2019) Preparation process optimization of pig bone collagen peptide-calcium chelate using response surface methodology and its structural characterization and stability analysis. *Food Chem* 284:80–89. <https://doi.org/10.1016/j.foodchem.2019.01.103>
 46. Singh P, Benjakul S, Maqsood S, Kishimura H (2011) Isolation and characterisation of collagen extracted from the skin of striped catfish (*Pangasianodon hypophthalmus*). *Food Chem* 124(1):97–105. <https://doi.org/10.1016/j.foodchem.2010.05.11>
 47. Wang S, Sun X, Zhou D (2017) Physicochemical characteristics and fibril-forming properties of collagen from paddlefish (*Polyodon spathula*) and globefish (*Fugu flavidus*) skin byproducts. *Food Sci Technol* 37:176–183

48. Kozłowska J, Sionkowska A, Skopinska-Wisniewska J, Piechowicz K (2015) Northern pike (*Esox lucius*) collagen: extraction, characterization and potential application. *Int J Biol Macromol* 81:220–227. <https://doi.org/10.1016/j.ijbiomac.2015.08.002>
49. Sun L, Li B, Song W, Si L, Hou H (2017) Characterization of Pacific cod (*Gadus macrocephalus*) skin collagen and fabrication of collagen sponge as a good biocompatible biomedical material. *Process Biochem* 63:229–235. <https://doi.org/10.1016/j.procbio.2017.08.003>
50. Bhuimbar MV, Bhagwat PK, Dandge (2019) Extraction and characterization of acid soluble collagen from fish waste: development of collagen-chitosan blend as food packaging film. *J Environ Chem Eng* 7:102983. <https://doi.org/10.1016/j.jece.2019.102983>
51. Slimane E, Sadok S (2018) Collagen from cartilaginous fish by-products for a potential application in bioactive film composite. *Molecules* 16:211. <https://doi.org/10.3390/md16060211>
52. Zou Y, Wang L, Cai P, Li P, Zhang M, Sun Z, Sun C, Xu W, Wang D (2017) Effect of ultrasound assisted extraction on the physicochemical and functional properties of collagen from soft-shelled turtle calipash. *Int J Biol Macromol* 105:1602–1610. <https://doi.org/10.1016/j.ijbiomac.2017.03.011>
53. Iswariya S, Velswamy P, Uma TS (2018) Isolation and characterization of biocompatible collagen from the skin of puffer fish (*Lagocephalus inermis*). *J Polym Environ* 26:2086–2095. <https://doi.org/10.1007/s10924-017-1107-1>
54. Jiang H, Kong Y, Song L, Liu J, Wang Z (2023) A thermostable type I collagen from swim bladder of silver carp (*Hypophthalmichthys molitrix*). *Mar Drugs* 21:280. <https://doi.org/10.3390/md21050280>
55. Wahyu YI, Widjanarko SB (2018) Extraction optimization and characterization of acid soluble collagen from milkfish scales (*Chanos chanos* Forskal). *Carpathian J Food Sci Technol* 10(1):125–135
56. Arumugam GKS, Sharma D, Balakrishnan RM, Ettiyappan JBP (2018) Extraction, optimization and characterization of collagen from sole fish skin. *Sustain Chem Pharm* 9:19–26. <https://doi.org/10.1016/j.scp.2018.04.003>
57. Melacini G, Bonvin AMJJ, Goodman M, Boelens R, Kaptein R (2000) Hydration dynamics of the collagen triple helix by NMR. *J Mol Biol* 300(5):1041–1048. <https://doi.org/10.1006/jmbi.2000.3919>
58. Zhang X, Jia Q, Li M, Liu H, Wang Q, Wu Y, Niu L, Liu Z (2021) Isolation of a novel calcium-binding peptide from phosvitin hydrolysates and the study of its calcium chelation mechanism. *Food Res Int* 141:110169. <https://doi.org/10.1016/j.foodres.2021.110169>
59. Abinaya M, Gayathri M (2019) Biodegradable collagen from *Scomberomorus lineolatus* skin for wound healing dressings and its application on antibiofilm properties. *J Cell Biochem* 120:15572–15584. <https://doi.org/10.1002/jcb.28824>
60. Krishnamoorthi J, Ramasamy P, Shanmugam V, Shanmugam A (2017) Isolation and partial characterization of collagen from outer skin of *Sepia pharaonis* (Ehrenberg, 1831) from Pudukkottai coast. *Biochem Biophys Rep* 10:39–45. <https://doi.org/10.1016/j.bbrep.2017.02.006>
61. Montoya MH, Arias JL, Plascencia M, Santacruz H, Rouzaud O, Cardenas JL, Marquez E, Ezquerro JM (2010) Jumbo squid (*Dosidicus gigas*) mantle collagen: extraction, characterization, and potential application in the preparation of chitosan-collagen biofilms. *Bioresour Technol* 101:4212–4219. <https://doi.org/10.1016/j.biortech.2010.01.008>
62. Tamilmozhi S, Veeruraj A, Arumugam M (2013) Isolation and characterization of acid and pepsin-solubilized collagen from the skin of sailfin (*Istiophorus platypterus*). *Food Res Int* 54:1499–1505. <https://doi.org/10.1016/j.foodres.2013.10.002>
63. Nurilmala M, Hizbullah H, Karnia E, Kusumaningtyas E, Ochiai Y (2020) Characterization and antioxidant activity of collagen, gelatin, and the derived peptides from yellowfin tuna (*Thunnus albacares*) skin. *Mar Drugs* 18:98. <https://doi.org/10.3390/md18020098>
64. Ša R, Martin B, Milon H, Tomás S, Vöröš D (2021) The proportion of the key components analysed in collagen-based isolates from fish and mammalian tissues processed by different protocols. *J Food Compos Anal* 103:104059. <https://doi.org/10.1016/j.jfca.2021.104059>
65. Felician F, Xia C, Qi W, Xu H (2018) Collagen from marine biological sources and medical applications. *Chem Biodivers* 15:1700557. <https://doi.org/10.1002/cbdv.201700557>
66. Minh T, Le T, Osako K, Nguyen VM, Truc T, Kigen T (2020) Comparison of acid-soluble collagen characteristic from three important freshwater fish skins in Mekong Delta Region. *Vietnam J Food Biochem* 44:1–8. <https://doi.org/10.1111/jfbc.13397>
67. Nurilmala M, Fauzi S, Mayasari D, Batubar I (2019) Collagen extraction from yellowfin tuna (*Thunnus albacares*) skin and its antioxidant activity. *J Teknol* 81:141–149. <https://doi.org/10.11113/jt.v81i1.11614>
68. Song W, Liu D, Sun L, Li B, Hou H (2019) Physicochemical and biocompatibility properties of Type I collagen from the skin of Nile tilapia. *Molecules* 17:137. <https://doi.org/10.3390/md17030137>
69. Grube M, Cinar G, Schubert US, Nischang I (2020) Incentives of using the hydrodynamic invariant and sedimentation parameter for the study of naturally and synthetically-based macromolecules in solution. *Polymers* 12:277. <https://doi.org/10.3390/polym12020277>
70. León-López A, Morales-Peñalosa A, Martínez-Juárez VM, Vargas-Torres A, Zeugolis DI, Aguirre-Álvarez G (2019) Hydrolyzed collagen-sources and applications. *Molecules* 24:1–16. <https://doi.org/10.3390/molecules24224031>
71. Grønlien KG, Pedersen ME, Sanden KW, Høst V, Karlsen J, Tønnesen HH (2019) Collagen from Turkey (*Meleagris gallopavo*) tendon: a promising sustainable biomaterial for pharmaceutical use. *Sustain Chem Pharm* 13:100166. <https://doi.org/10.1016/j.scp.2019.100166>
72. Ahmed R, Haq M, Chun BS (2019) Characterization of marine derived collagen extracted from the by-products of bigeye tuna (*Thunnus obesus*). *Int J Biol Macromol* 135:668–676. <https://doi.org/10.1016/j.ijbiomac.2019.05.213>
73. Soroushanova A, Delgado LM, Wu Z, Shologu N, Kshirsagar A, Raghunath R, Mullen AM, Bayon Y, Pandit A, Raghunath M, Zeugolis DI (2018) The collagen suprafamily: from biosynthesis to advanced biomaterial development. *Adv Mater* 31:1–39. <https://doi.org/10.1002/adma.201801651>
74. Diogo GS, Carneiro F, Freitas-Ribeiro S, Sotelo CG, Pérez-Martín RI, Pirraco RP, Reis RL, Silva TH (2021) Prionace glauca skin collagen bioengineered constructs as a promising approach to trigger cartilage regeneration. *Mater Sci Eng C* 120:111587. <https://doi.org/10.1016/j.msec.2020.111587>
75. Andonegi M, Peñalba M, de la Caba K, Guerrero P (2020) ZnO nanoparticle-incorporated native collagen films with electroconductive properties. *Mater Sci Eng C* 108:110394. <https://doi.org/10.1016/j.msec.2019.110394>
76. Cheng X, Shao Z, Li C, Yu L, Raja MA, Liu C (2017) Isolation, characterization and evaluation of collagen from jellyfish *Rhopilema esculentum* kishinouye for use in hemostatic applications. *PLoS ONE* 12:1–21. <https://doi.org/10.1371/journal.pone.0169731>
77. Chen J, Li M, Yi R, Bai K, Wang G, Tan R (2019) Electrodialysis extraction of pufferfish skin (*Takifugu flavidus*): a promising

- source of collagen. *Mar Drugs* 17:25. <https://doi.org/10.3390/md17010025>
78. Asaduzzaman AKM, Getachew AT, Cho YJ, Park JS, Haq M, Chun BS (2020) Characterization of pepsin-solubilised collagen recovered from mackerel (*Scomber japonicus*) bone and skin using subcritical water hydrolysis. *Int J Biol Macromol* 148:1290–1297. <https://doi.org/10.1016/j.ijbiomac.2019.10.104>
79. He M, Shi L, Wang G, Cheng Z, Han L, Zhang X, Wang C, Wang J, Zhou P, Wang G (2019) Biocompatible and biodegradable chitosan/sodium polyacrylate polyelectrolyte complex hydrogels with smart responsiveness. *Int J Biol Macromol* 155:1245–1251. <https://doi.org/10.1016/j.ijbiomac.2019.11.092>
80. Wang X, Gao A, Chen Y, Zhang X, Li S, Chen Y (2017) Preparation of cucumber seed peptide-calcium chelate by liquid state fermentation and its characterization. *Food Chem* 229:487–494. <https://doi.org/10.1016/j.foodchem.2017.02.121>
81. Song X, Wang Z, Tao S, Li G, Zhu J (2017) Observing effects of calcium/magnesium ions and pH value on the self-assembly of extracted swine tendon collagen by atomic force microscopy. *J Food Qual.* <https://doi.org/10.1155/2017/9257060>
82. Mccarthy EM, Floyd H, Addison O, Zhang ZJ, Oppenheimer PG, Grover LM (2018) Influence of cobalt ions on collagen gel formation and their interaction with osteoblasts. *Am Chem Soc Omega* 3:10129–10138. <https://doi.org/10.1021/acsomega.8b01048>
83. Sorushanova A, Coentro JQ, Pandit A, IZeugolis D, Raghunath M (2017) 2.15 Collagen: materials analysis and implant uses. *Comprehensive Biomaterials II*:332–350
84. Yue C, Ding C, Yang N, Luo Y, Su J, Cao L, Cheng B (2022) Strong and tough collagen/cellulose nanofibril composite films via the synergistic effect of hydrogen and metal–ligand bonds. *Eur Polym J* 180:111628. <https://doi.org/10.1016/j.eurpolymj.2022.111628>
85. Pang X, Sun P, Tan Z, Lin L, Tang B (2016) Effect of calcium ions on the nanostiffness of articular cartilage. *Mater Lett* 180:332–335. <https://doi.org/10.1016/j.matlet.2016.05.158>
86. Ling Z, Gu J, Liu W, Wang K, Huang C, Lai C, Yong Q (2020) Actuating, shape reconstruction, and reinforcement of galactomanan-based hydrogels by coordination bonds induced metal ions capture. *Int J Biol Macromol* 165:2721–2730. <https://doi.org/10.1016/j.ijbiomac.2020.10.059>
87. Shaheen A, Maswal M, Dar AA (2021) Synergistic effect of various metal ions on the mechanical, thixotropic, self-healing, swelling and water retention properties of bimetallic hydrogels of alginate. *Colloids Surfaces A* 627:127223. <https://doi.org/10.1016/j.colsurfa.2021.127223>
88. Huang Y, Xiao L, Zhou J, Liu T, Yan Y, Long S, Li X (2021) Strong tough polyampholyte hydrogels via the synergistic effect of ionic and metal–ligand bonds. *Adv Funct Mater.* <https://doi.org/10.1002/adfm.202103917>
89. Pang X, Lin L, Tang B (2017) Unraveling the role of Calcium ions in the mechanical properties of individual collagen fibrils. *Sci Rep* 7:1–8. <https://doi.org/10.1038/srep46042>
90. Wang Q, Zhang L, Liu Y, Zhang G, Zhu P (2019) Characterization and functional assessment of alginate fibers prepared by metal-calcium ion complex coagulation bath. *Carbohydr Polym.* <https://doi.org/10.1016/j.carbpol.2019.115693>
91. Wang S, Lv Y, Feng S, Li Q, Zhang T (2018) Bimetallic ions synergistic cross-linking high-strength rapid self-healing antibacterial hydrogel. *Polym Eng Sci* 59:919–927. <https://doi.org/10.1002/pen.25037>
92. Wei Z, Duan H, Weng G, He J (2020) Metals in polymers: hybridization enables new functions. *J Mater Chem C* 8:15956–15980. <https://doi.org/10.1039/d0tc03810e>
93. Cunha C, Klumpers D, Li W, Koshy S, Weaver J, Chaudhuri O, Granja P, Mooney D (2014) Influence of the stiffness of three-dimensional alginate/collagen-I interpenetrating networks on fibroblast biology. *Biomaterials* 35(32):8927–8936. <https://doi.org/10.1016/j.biomaterials.2014.06.047>
94. Wang X, Zhang Z, Xu H, Li X, Hao X (2020) Calcium chelate using enzymolysis-fermentation methodology and its structural characterization and stability analysis. *RCS Adv* 10:11624–11633. <https://doi.org/10.1039/d0ra00425a>
95. Yang X, Yu X, Yagoub AEGA, Chen L, Wahia H, Osae R, Zhou C (2021) Structure and stability of low molecular weight collagen peptide (prepared from white carp skin)-calcium complex. *LWT* 136:110335. <https://doi.org/10.1016/j.lwt.2020.110335>
96. Sun N, Wang Y, Bao Z, Cui P, Wang S, Lin S (2019) Calcium binding to herring egg phosphopeptides: binding characteristics, conformational structure and intermolecular forces. *Food Chem.* <https://doi.org/10.1016/j.foodchem.2019.125867>
97. Ye Q, Wu X, Zhang X, Wang S (2019) Function soybean peptide-selenium and its functional. *Foods Funct* 10:4761–4770. <https://doi.org/10.1039/c9fo00729f>
98. Oliveira VM, Neri RCA, Monte FTD, Roberto NA, Costa HMS, Assis CRD, Santos JF, Bezerra RS, Porto ALF (2019) Crosslink-free collagen from *Cichla ocellaris*: structural characterization by FT-IR spectroscopy and densitometric evaluation. *J Mol Struct* 1176:751–758. <https://doi.org/10.1016/j.molstruc.2018.09.023>
99. Wu W, Jia J, Wen C, Yu C, Zhao Q, Hu J (2021) Optimization of ultrasound assisted extraction of abalone viscera protein and its effect on the iron-chelating activity. *Ultrason Sonochem* 77:105670. <https://doi.org/10.1016/j.ultsonch.2021.105670>
100. Zhang H, Zhao L, Shen Q, Qi L, Jiang S, Guo Y, Zhang C, Richel A (2021) Preparation of cattle bone collagen peptides-calcium chelate and its structural characterization and stability. *LWT* 144:111264. <https://doi.org/10.1016/j.lwt.2021.111264>

Publisher's Note Springer Nature remains neutral with regard to jurisdictional claims in published maps and institutional affiliations.